ELSEVIER

Sensors and Actuators A 94 (2001) 19–24

SENSORS AND ACTUATORS A PHYSICAL

www.elsevier.com/locate/sna

Load characterization of high displacement piezoelectric actuators with various end conditions

James Mulling, Tim Usher[1], Brian Dessent, Jeremy Palmer, Paul Franzon, Eddie Grant, Angus Kingon*

Materials Research Center, North Carolina State University, Campus Mail Box 7919, Raleigh, NC 27695-7919, USA

Received 19 May 2000; accepted 5 February 2001

Abstract

Piezoelectric ceramic transducers are characterized by relatively small strains on the order of 0.1%. One method of achieving significantly larger displacements is to utilize flexural mode actuators, such as unimorphs or bimorphs. In this paper, we investigate a particular type of stressed unimorph flexural actuator, viz. the 'THUNDER' actuators. (THUNDER^{TM} is a trademark of Face International Corporation). These stressed unimorphs are of interest due to their particularly large flexural strains. To determine their versatility as high displacement actuators, it was necessary to investigate their actuation capability as a function of load. In addition, our investigation determined that end conditions have an appreciable effect, which has also not been reported in the literature. Therefore, experimental results of the load capabilities of these high displacement actuators with various end conditions are presented here. Commercially available rectangular actuators were chosen for this study. The actuators had been constructed by bonding thin PZT ceramics (0.152 mm thick, 1.37 cm wide, 3.81 cm long) to stainless steel sheets (0.20 mm thick, 1.27 cm wide, 6.35 cm long). They were operated in a flexural mode. It was shown that progressively restrictive end conditions increased the stiffness, ranging from 2.5 to 23 N/m, enhancing the load capabilities of the actuator. In some cases, displacement actually increased as a function of load. This enhanced stiffness was obtained at a cost of reduced no load flexural strain (defined as the ratio of flexural displacement and ceramic length), ranging from 1.08% for free-end conditions to 0.2% for highly restricted end conditions. The load bearing capabilities were tested out to 10 N for most end conditions.

Keywords: THUNDER transducers; Piezoelectric; Actuator; Ferroelectric; PZT; Unimorph

1. Introduction

Piezoelectric actuators are manufactured in many forms. Simple devices include disc multilayers (also known as stacks), and simple cylinders [1]. More complex devices include unimorphs, bimorphs, moonies, hinged levers and inchworms [2]. Typical piezoelectric actuators have strains on the order of 0.1%, which severely limits their applicability. Traditionally, this problem has been addressed by utilizing the high strain capabilities of piezoelectrics, along with an external mechanical advantage mechanism to produce larger displacements. More recently, composite structures have been produced. The first structure of this type was called RAINBOW. A subsequent structure is known as THUNDER^{TM}. These materials can have flexural strains on the order of 1%, which are a full order of magnitude higher than typical piezoelectrics. The flexural strain is defined as the flexural displacement divided by the length of the ceramic. These ultra high displacements are strongly dependent on physical boundary conditions. The current literature contains virtually no information on this dependency. A thorough investigation of load capabilities is also absent from the literature.

In 1994, Haertling [3] introduced a new type of transducer/actuator, which he called reduced and internally biased oxide wafer (RAINBOW). The actuator is formed by reducing one side of a lead lanthanum zirconate titanate (PLZT) disk at high temperature, thereby transforming a surface layer from ceramic to a nearly metallic composition. Upon cooling, the disk deforms to a characteristic, shallow dome shape due to a difference in coefficients of expansion between the reduced layer and the bulk of the ceramic. Actuator fabrication is completed by poling perpendicular to the piezoelectric/metallic interface. These actuators pro-

* Corresponding author. Tel.: +1-919-515-8636; fax: +1-919-515-3149.
E-mail address: angus_kingon@ncsu.edu (A. Kingon).
[1] Permanent address: Department of Physics, California State University at San Bernardino, San Bernardino, CA, USA.

0924-4247/01/$ – see front matter © 2001 Published by Elsevier Science B.V.
PII: S0924-4247(01)00688-4

duced flexural strains of 0.5% where the diameter (22.4 cm) was used in the case of disk actuators.

The thin-layer composite unimorph ferroelectric driver and sensor (THUNDER^{TM}) actuator [4], developed under grants from NASA, achieves deformation and pre-stress by a different route. A lead zirconate titanate (PZT) ceramic thin sheet is bonded under hydrostatic pressure to a metal substrate *while at* elevated temperature. Upon cooling, the laminate develops curvature and consequent internal stresses due to differences in coefficients of expansion between the metal layer and ceramic layer. As with RAINBOWs, actuator fabrication is completed by poling perpendicular to the piezoelectric/metal interface.

When compared, the RAINBOW and THUNDER^{TM} show many similarities. The fabrication methods, however, are very different. Wise [6] reports that free displacements were 10–25% higher for RAINBOWs. However, the THUNDER^{TM} actuators are very rugged, and standard commercial manufacturing techniques have been developed. To our knowledge, no such manufacturing techniques have been developed for RAINBOWs.

It is important to realize that when compared to more traditional piezoelectric actuators, these high displacement actuators operate very differently. The actuators can operate in one of several modes. The mode described below is the one we found most useful for our application. As explained above, the manufacturing process results in an arc or dome shape that introduces asymmetry. Consider an actuator placed on a horizontal surface such that its convex side is facing upward. Now, consider a voltage applied across the thin dimension of the ceramic with the top being more positive than the bottom. The ceramic tends to contract because of the negative d_{31} transverse coupling. The result is that the actuator becomes flatter. The apex of the arc moves downward. This lower position of the apex is the reference from which displacements are measured. Now, if the voltage is released, the actuator returns to its original position. The distance from the flatter reference point to this final point is the free displacement. Now, if a mass is placed at the apex of the arc or dome the loaded actuator tends to flatten. If a voltage is applied, the apex point moves even further downward. This is the new reference. Again the voltage is removed, and the apex moves upward. This is the displacement for that particular load. So, free displacement involves two steps. One step is a piezoelectric response to an applied voltage. The other step is a mechanical response. It may be useful to think of this type of actuator as a spring in which the stiffness can be altered with an external voltage. With no applied voltage, the actuator compresses just like a leaf spring when a load is placed on it. If a voltage is applied while the load is on it, the actuator becomes stiffer, resulting in a positive y displacement (y is measured in the downward direction) of the load. A more detailed explanation, specific to our experimental conditions, will be given later.

While displacement data and limited force data are available in the literature [5,6], reported results generally assume that the THUNDER^{TM} actuators are ''simply supported'', that is, resting on a pair of knife edges, or attached to supports by flexible media such as duct tape or modeling clay. This article reports results obtained by controlling boundary conditions more carefully, so that the effects of hindered or allowed rotation or translation on one or both ends of a THUNDER^{TM} actuator can be examined.

2. Procedure

Commercially available THUNDER^{TM} actuators [7] were used in this investigation. The specifications are given in Table 1. The experimental apparatus is shown in Fig. 1. The actuators were installed in a fixture designed to control specifically whether actuator ends were free to rotate or translate in various combinations of end conditions. This fixture and accompanying apparatus are shown in Fig. 1. Each end of an actuator is clamped into an axle.

The axles are free to rotate unless bolted. One axle is mounted in a socket slightly elongated in the horizontal direction. This arrangement allows translation during actuator flexure unless a bolt is inserted to block translation. Allowing translation in both axles is redundant and adds unnecessary complication to the test fixture. A linear variable differential transformer (LVDT) for measuring changes in position of the actuator surface at its center is mounted in a frame positioned above the actuator fixture. The LVDT core is connected to a steel shaft constrained by a linear bearing at its lower end. Slotted weights can be stacked against the intermediate portion of the shaft, supported by an enlarged section of shaft, thus enabling application of variable loads to an actuator.

Based on its design, the test fixture blocks or allows rotation in the left axle, right axle, or both axles. The means for allowing or blocking translation was available only in the right axle. In general, a decision tree of three variables two deep (rotation right — yes or no, rotation left — yes or no, translation — yes or no) generates eight permutations, but blocking rotation in the right axle also effectively blocks its translation. However, blocking *translation* of the right axle did not block its rotation. Thus, two of the eight permutations are omitted, and the effect of end conditions on actuator performance was evaluated for the end conditions summarized in Table 2.

Table 1
Dimensions of TH 8-R THUNDER^{TM} actuator

Substrate	Stainless steel
Thickness	0.152 mm (6 mil)
Width	1.37 cm (0.540 in.)
Length	6.35 cm (2.5 in.)
Ceramic	PZT-5A
Thickness	0.20 mm (8 mil)
Width	1.27 cm (0.5 in.)
Length	3.81 cm (1.5 in.)

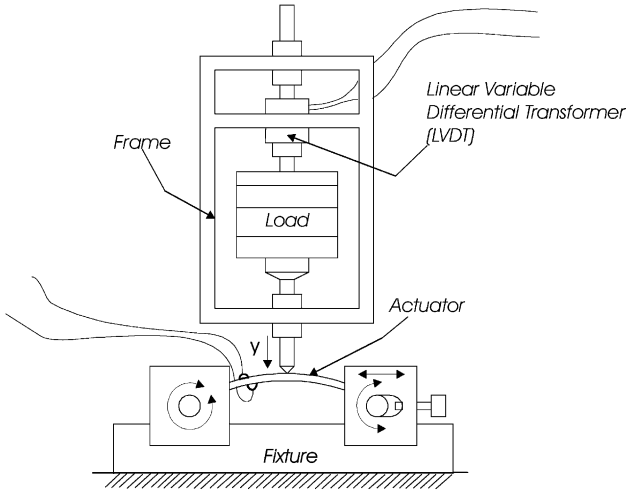

Fig. 1. Test apparatus for measuring actuator positions under various loads at a range of applied voltages and various end conditions. The fixture shown in the lower portion allows free rotation of each end and free horizontal translation of one end as indicated by the arrows. Each of these end conditions can be blocked. The positive y direction is taken to be downward. The frame shown in the upper portion of the apparatus is externally supported (not shown). The central rod rests on the curved actuator. The rod extends upward through a linear bearing in the lower portion of the frame. Slotted weights are placed on an enlarged section of shaft located above the linear bearing. A LVDT located in the upper portion of the frame senses the position of the rod.

The following is a more specific description of the actuation mechanism given in the introduction. The indirect means by which THUNDER^{TM} actuators generate mechanical displacement is less straightforward than the displacement of a piezoelectric stack. As a pre-stressed, composite beam with negative curvature (the shape of a shallow arch), the structure deflects toward flatness under applied load. Upon electrical excitation, the upper piezoelectric layer contracts in the direction orthogonal to its poling direction — parallel to its surface. This introduces internal stresses that act in the same direction as those generated by loading, thus producing an additional increment of deflection toward flatness. When electrical excitation is stopped, the actuator displacement is greater than is appropriate for the applied load. The elastic rebound results in sudden displacement back to its initial position. Typical free displacements range from 300 to 400 μm for an applied voltage of 450 V and free end conditions.

The rebound step in the displacement cycle, which typically does work against a load, is purely an elastic response, rather than an electrically-driven movement. While it is possible to drive the THUNDER^{TM} actuator under reversed polarity, voltage must be limited to avoid damage to the actuator. This limits the usefulness of reversed polarity operation.

Data from each test were automatically acquired in conjunction with a LabVIEW computer program, which determined measurement range under each condition, then acquired and averaged 20,000 points for each measurement. To calibrate the relationship between LVDT signal and actuator position, a scaling factor (μm/mV or equivalently, mm/V) was determined, using a number of reference thicknesses.

Careful attention was paid to repeatability. For every end condition, six full data sets were repeated without changing anything about the test arrangement. The average and deviation were then plotted as a function of load. In each end condition, the first data set of the six taken showed a statistically significant variation from the other five data sets. The average displacement in the first set was always higher than in the remaining five. After numerous investigations eliminated such things as electronic drift and ferroelectric relaxation, the phenomenon was attributed to mechanical settling in the test apparatus. In every series, the five data sets other than the first did not show any significant differences. Later, some of the same end conditions were repeated with different actuators with no significant difference detected.

Table 2
Table of six end conditions for all the allowed combinations[a]

End condition	Right	Left	Translation
A	Y	Y	Y
B	Y	N	Y
C	Y	Y	N
D	N	Y	N
E	Y	N	N
F	N	N	N
Omit	N	Y	Y
Omit	N	N	Y

[a] The end conditions range from complete freedom of both translation and rotation to total restriction of both rotation and translation.

3. Results

Fig. 2 shows a plot of position versus load for end condition A, in which translation and rotation of each end is allowed (see Table 2). Note that positive position is downward and measured in reference to minimal load and no voltage. Straight lines are fitted through some of the data points. The lower line is drawn through zero voltage data points, and shows the inherent stiffness of the actuator as a passive beam. The upper line is drawn through the highest voltage (480 V) data points. The difference in slopes between these two lines demonstrates a voltage-dependent stiffness. Other lines connecting similar voltage levels have been omitted for clarity.

Fig. 3 shows a plot of displacement versus load data for the same end condition as in Fig. 2. Displacement is defined as the difference between the zero voltage position and the position of the actuator with 480 V applied. In the graphs, the displacement is referenced to zero voltage for each applied load. We were careful to distinguish between movement due to the inherent (zero applied voltage) compliance of the

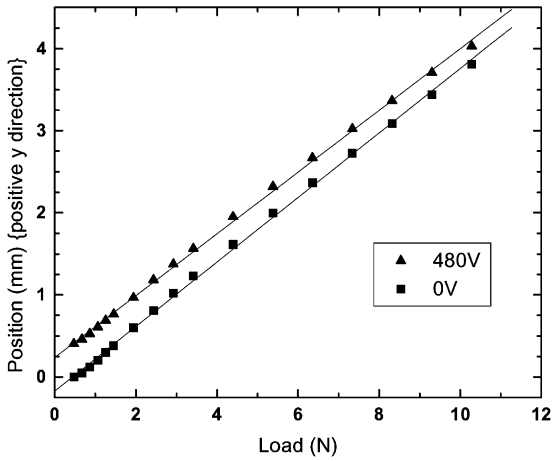

Fig. 2. Experimental data for end condition A in which translation, and rotation of both axles were allowed. Ten different voltages ranging from 0 to 480 V were applied to the actuator. The upper line is drawn through data points corresponding to 480 V, whereas the lower line is drawn through 0 V. Data points corresponding to intermediate voltages were omitted for clarity. The position is referenced to zero load and zero voltage for all data. The different slopes show the voltage dependence of the actuator stiffness.

actuator and the voltage induced movement. Each plotted position or displacement value represents the average of values (for the particular load and voltage) from the five data sets (omitting the first data set) generated under each end condition.

Actuator displacement was greatest at all loads in the unconstrained end conditions (both rotation and translation allowed at both ends of actuator). Data plotted in Fig. 3, indicates a maximum displacement of 410 μm at no load, falling to 237 μm under the maximum load (exerted by the mass (kg) plus support rod) just above 10 N. Since the spacing decreases between lines for increasing voltage

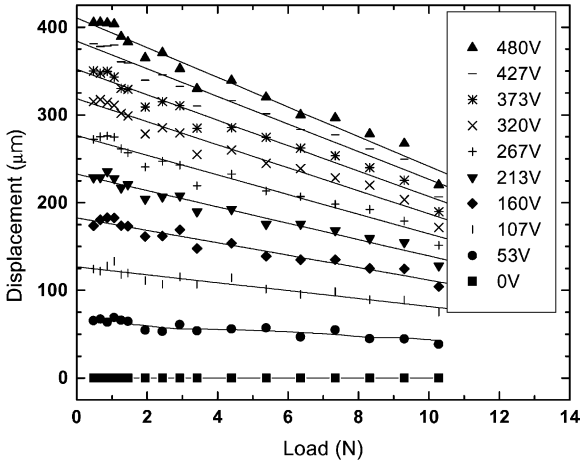

Fig. 3. The same data as shown in Fig. 2 is plotted here, however the displacement (as opposed to the position) is shown on the vertical axis. The displacement is referenced to zero voltage for each applied load. Information about the voltage-dependent stiffness is obscured but a clearer view of the usable displacement for a constant load is obtained.

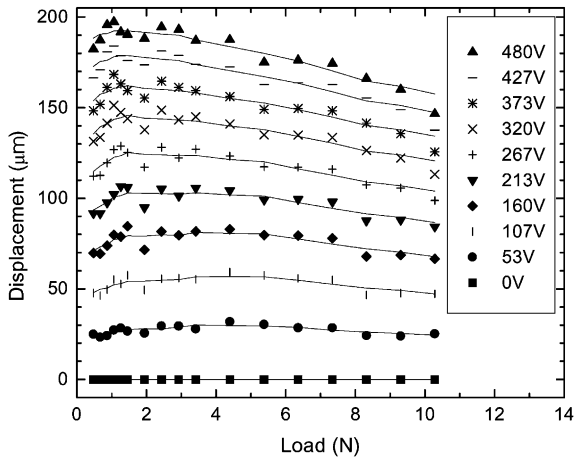

Fig. 4. Experimental data for end condition B in which the rotation of one axle is blocked. Translation and the rotation of the other axle are allowed. The no-load displacement is reduced by approximately one-half as compared to completely free end condition.

levels, it is evident that increasing toward the maximum operating voltage (480 V) generates decreasing returns in the form of greater displacement.

The effect of introducing even a small end constraint is evident from data for end condition D, in which only rotation in one axle has been blocked. Data plotted in Fig. 4 indicate that no load displacement has fallen to approximately half that for the unconstrained end condition. This represents increased structural stiffness. Note, however, that the negative slope of fitted lines in Figs. 3 and 4 indicates that displacement decreases with increasing load under the relatively free-end conditions.

As actuator ends are further constrained, the reduction of displacement in return for increased stiffness continues, but successive further constraints have diminishing effect. Data plotted in Fig. 5 indicates that no load displacement has fallen to 80 μm. Thus, the effect of blocking translation is greater that of blocking rotation. When both rotation and translation are blocked, the minimum level of no load displacement is approximately 60 μm.

When translation is blocked (rotation might also be blocked), an *increase* in displacement is observed with increasing load. This effect can be seen in Fig. 5. Eventually, a point of instability is reached and the actuator buckles. The buckling phenomenon is an abrupt transition or collapse from negative curvature (concave downward) to positive curvature (concave upward). Even an unconstrained actuator may flatten under high loads and then sag into a positive curvature as additional load applied. However, the transition is a gradual settling, not a sudden and abrupt collapse. Fig. 5 has been truncated beyond an applied load of 7 N and does not show data through the buckling transition. However, a non-linearity at the high-load ends of the fitted lines indicates that buckling is imminent.

Finally, a summary is presented in Fig. 6, which maps measurements taken at each end condition on a stiffness

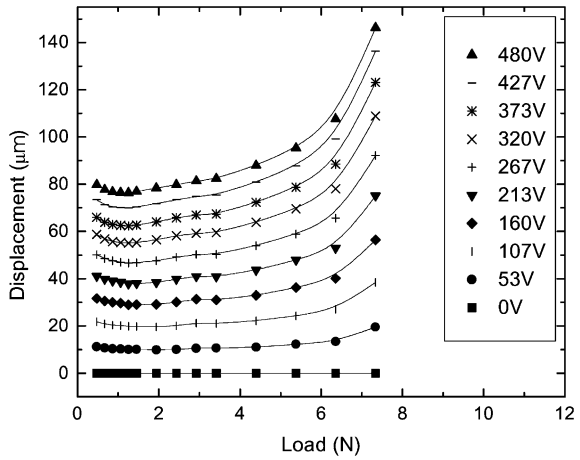

Fig. 5. Experimental data for end condition F in which translation and rotation of both axles are blocked. The no-load displacement is further reduced as compared to end condition B shown in Fig. 4. In contrast to end conditions A and B shown in Figs. 3 and 4, respectively, the displacement increases with increasing load, becoming non-linear at higher loads indicating the onset of buckling.

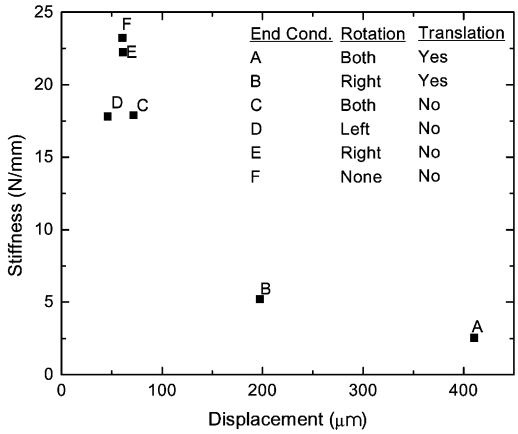

Fig. 6. A summary of the experimental data, showing the reciprocal relation between stiffness and no load displacement. The unconstrained end conditions appear in the lower right portion. More constrained end conditions are represented in the upper left corner. Repeated or symmetric end conditions are represented by the same symbol.

versus displacement plane. Measurements on unconstrained actuators result in a point in the zone of high displacement and low stiffness. An intermediate point from end condition D, where rotation of the right axle was the only restraint, is plotted at approximately half the displacement and twice the stiffness of unconstrained actuator data. Several points characterized by blocked translation fall in the zone of high stiffness and low displacement. The plotted points approximately follow a hyperbolic trace, that is, the product of stiffness and displacement remains approximately constant when end conditions are modified. This can be verified by multiplying same-row values from columns in Table 3 for ''no load displacement'' and ''stiffness at 0 V'', which corresponds to Fig. 6.

The data in Table 3 show correlation between percent change in actuator stiffness due to applied voltage, the trend of either increasing or decreasing displacement with increasing load, and degree of constraint from end conditions. Note that displacement increased with increasing load when translation was blocked, with the exception of end condition B. In this case, rotation and translation were not blocked on the same axle. We believe some asymmetry in the test fixture allowed this configuration to produce a slightly lower degree of constraint than for end condition D, where rotation and translation have been blocked on the same axle. Otherwise, the two end conditions were symmetrical and should have given nearly the same results.

Likewise, values in the column for ''percent stiffness'' change positively under end conditions which allow translation, and negatively when translation is blocked, again with the exception of end condition B. Percent change was calculated by subtracting 0 V stiffness from 480 V stiffness and dividing by the average of the two. Note also that stiffness values given in Table 3 are the inverse of the slopes of fitted lines in graphs included in this report simply because the graphs are more easily interpreted by viewing displacement as the response to a given load. The slope values would give compliance rather than stiffness.

In summary, end conditions involving blocked translation or higher degrees of constraint tended to result in increased stiffness (lower downward displacement) with applied voltage and with increasing displacement with increasing load. The last aspect suggests that constrained actuators do more work as load increases. Calculations of load/displacement

Table 3
Summary table relating end conditions with stiffness and displacement

Description			Strain (%)			Stiffness (N/mm)		
End condition	Rotation	Translation	No load	10 N	Increasing/decreasing with load	0 V	480 V	Change (%)
A	Both	Yes	1.08	0.634	Decreases	2.55	2.66	4.39
B	Right	Yes	0.518	0.416	Decreases	5.22	5.32	2.04
C	Both	No	0.188	0.305	Increases	17.9	16.6	−7.68
D	Left	No	0.121	0.324	Increases	14.9	13.4	−10.9
E	Right	No	0.160	0.254	Increases	22.2	20.6	−7.66
F	None	No	0.159	0.187	Increases	23.2	22.7	−2.50

work performed support this, although other experiments have shown that the actuators must operate in a continuously loaded state, as in these tests, rather than seeing their load intermittently, as in inchworm devices, for higher work output to occur.

4. Concluding remarks

New high displacement piezoelectric actuators differ from more traditional actuators in many ways. It is important to understand and carefully characterize these differences. Two interdependent properties were reported here: end conditions and load capabilities. These two properties have important implications for applications. Our results show that if maximum free displacements are desired, care must be taken to remove end conditions on rotation and translation as much as possible. In the case of loaded actuation, constraining the end conditions results in a stiffer actuator, therefore enhanced load capabilities, but at the cost of smaller free displacement. In particular, blocking end translation substantially reduces free displacement and increases stiffness, more so than blocking end rotation. In addition, the buckling phenomenon is favored more by blocking translation than rotation. With translation blocked, the actuator displaces less in response to an applied load (increased stiffness), but collapses into the inverted curvature abruptly, which was our definition of buckling.

The effect of end conditions provides an option for increasing beam actuator stiffness. Either the laminate can be fabricated using a stiffer metal substrate, or the ends can be constrained, most effectively achieved by blocking translation. Within a load range below the buckling transition, an actuator with the property of increasing stiffness with increasing load could be obtained by blocking translation.

It is also important to realize that these new actuators have a different mode of operation when compared to more traditional actuators (for example, stacks). When acting against a load, the work is actually performed against the load when the voltage is released rather than when applied. (Stacks perform work when voltage is applied.) It may be useful to think of these actuators as springs with a voltage-controlled stiffness. Electrical excitation has the effect of increasing the stiffness of the actuator, therefore producing a displacement against the load. This introduces the interesting possibility of designing resonant mechanical systems, automotive suspensions for example, with a tunable resonant frequency. In mechanical systems, the stiffness and the mass determine the resonant frequency. In direct analogy, the capacitance and the inductance determine the resonant frequency of a tank circuit. In electrical circuits the capacitance and/or the inductance can easily be changed, resulting in a multitude of useful tuned circuit designs. In mechanical systems, the spring stiffness and mass are not easily changed. This type of actuator or ''voltage-controlled spring'' provides some control over the stiffness, therefore control over the resonant frequency.

Acknowledgements

The authors acknowledge support form DARPA, contract number N3998-98-C3536.

References

[1] K. Uchino, Piezoelectric Actuators and Ultrasonic Motors, Kluwer Academic Publishers, Dordrecht, 1997.
[2] Y. Sugawara, K. Onitsuka, S. Yoshikawa, Q.C. Xu, R.E. Newnham, K. Uchino, Metal–ceramic composite actuators, J. Am. Ceram. Soc. 75 (1992) 996–998.
[3] G.H. Haertling, Rainbow ceramics — a new type of ultra-high-displacement actuator, Bull. Am. Ceram. Soc. 73 (1994) 93–96.
[4] R.F. Hellbaum, R.G. Bryant, R.L. Fox, Thin layer composite unimorph ferroelectric driver and sensor, US patent no. 5632841 (1997).
[5] K.M. Mossi, G.V. Selby, R.G. Bryant, Thin-layer composite unimorph ferroelectric driver and sensor properties, Mater. Lett. 35 (1998) 39–49.
[6] S.A. Wise, Displacement properties of RAINBOW and THUNDER piezoelectric actuators, Sens. Actuators A 69 (1998) 33–38.
[7] Face International Norfolk, VA, USA (www.faceco.com).

Biographies

James Mulling, BS, Materials Science, North Carolina State University (NCSU), 1998. He is currently pursuing MS in Materials Science. He is a member of the microrobotics group at North Carolina State University (NCSU).

Tim Usher, PhD, University of South Carolina, 1990. He is an Associate Professor of Physics, California State University, San Bernardino and a member of the microrobotics group North Carolina State University (NCSU).

Brian Dessent, dual BS degrees in Electrical Engineering and Computer Engineering, NCSU, 1998, accepted into the graduate program at the University of California, Berkley. He is a member of the microrobotics group at North Carolina State University (NCSU).

Jeremy Palmer, BS degrees in Mechanical Engineering, 1994, University of Connecticut, currently pursuing a dual PhD in Electrical and Mechanical Engineering. He is a member of the microrobotics group at North Carolina State University (NCSU).

Paul Franzon PhD, 1988, University of Adelaide, Australia, Professor of Electrical and Computer Engineering at NCSU. He is a member of the microrobotics group at North Carolina State University (NCSU).

Eddie Grant PhD, 1999, University of Strathclyde, Glasgow, Scotland, UK, Associate Professor of Electrical and Computer Engineering and Director of the Center for Robotics and Intelligent Machines at NCSU. He is a member of the microrobotics group at North Carolina State University (NCSU).

Angus Kingon, PhD, 1981, University of South Africa, Professor of Materials Science and Engineering at NCSU. He is a member of the microrobotics group at North Carolina State University (NCSU).